

Supplementary Information for New Journal of Chemistry

Fabrication of Iron-Doped Fe@Zn-MOF Composite: Empowering Enhanced Colorimetric Recognition and Energy Storage Performance

Vibhav Shukla^a, Waris^b, Mohammad Zain Khan^b, Kafeel Ahmad Siddiqui^{a*}

^aDepartment of Chemistry, National Institute of Technology Raipur, G E Road Raipur – 492010, Chhattisgarh, India

^bDepartment of Applied Chemistry, Faculty of Engineering and Technology, ZHCET, Aligarh Muslim University, Aligarh, UP (India) – 202002

^a Corresponding Author: Dr. Kafeel Ahmad Siddiqui

^a e-mail: kasiddiqui.chy@nitrr.ac.in

Section S1. Selection of Solvents

We conducted a study on several solvents to better understand how well the as-produced Zn-MOF and Fe@Zn-MOF-2 can be detected. For fluorescence observations, a clear powder sample of Zn-MOF and Fe@Zn-MOF-2 (3 mg) was dissolved in 4 mL of various organic solvents, such as Ethanol (EtOH), Dimethyl sulfoxide (DMSO), Diethyl formamide (DEF), Tetrahydrofuran (THF), Chloroform (CHCl₃), Nitrobenzene (NB), Acetonitrile (CH₃CN), Methanol (MeOH), Dimethylformamide (DMF), water (H₂O), Acetone, and Iso-Propanol (i-Propanol). The mixture underwent a 30-minute ultrasonic treatment and was left undisturbed for 24 hours to maintain stable suspensions. Following exposure to 300 nm radiation, the suspension exhibited detectable fluorescence over the 200–600 nm range at room temperature. The solution of Zn-MOF and Fe@Zn-MOF-2 exhibited varying levels of fluorescence intensity, depending on the solvent used. Following stimulation at a wavelength of 300 nm, both the Zn-MOF and Fe@Zn-MOF-2

exhibited a remarkable emission intensity at 115 nm and 630 nm in ethanolic and aqueous solutions, respectively. Fig. S1 and S2 depict the intensity and quenching efficiencies of different solvents for Zn-MOF and Fe@Zn-MOF-2, respectively.

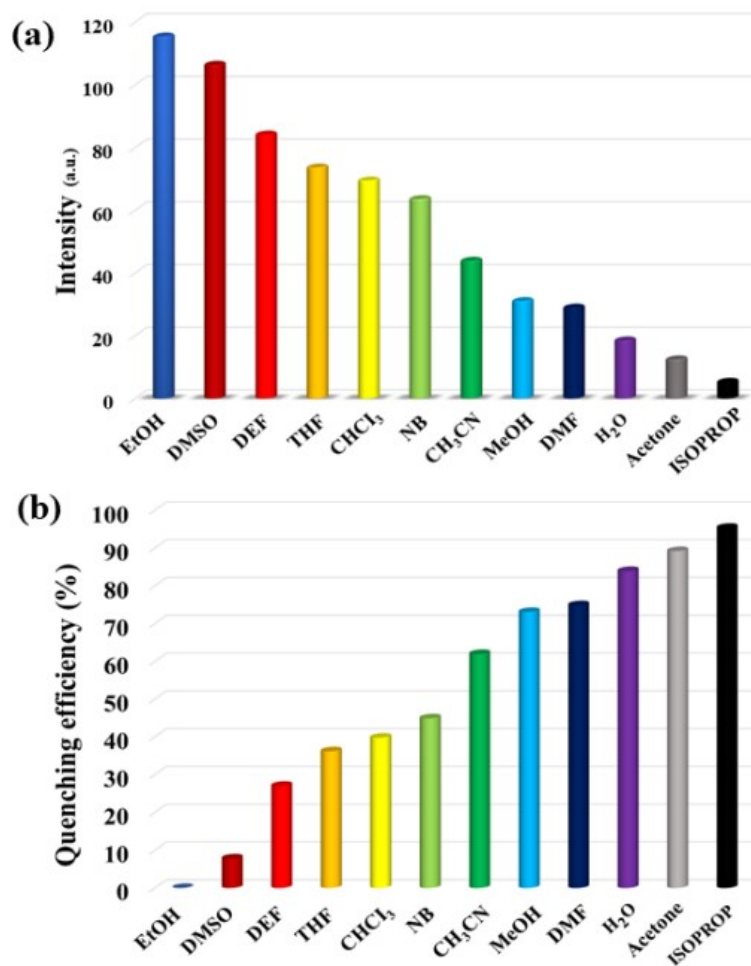


Fig. S1 For Zn-MOF (a) fluorescence intensity levels (b) quenching efficiencies, when numerous solvents are introduced when excited at 300 nm.

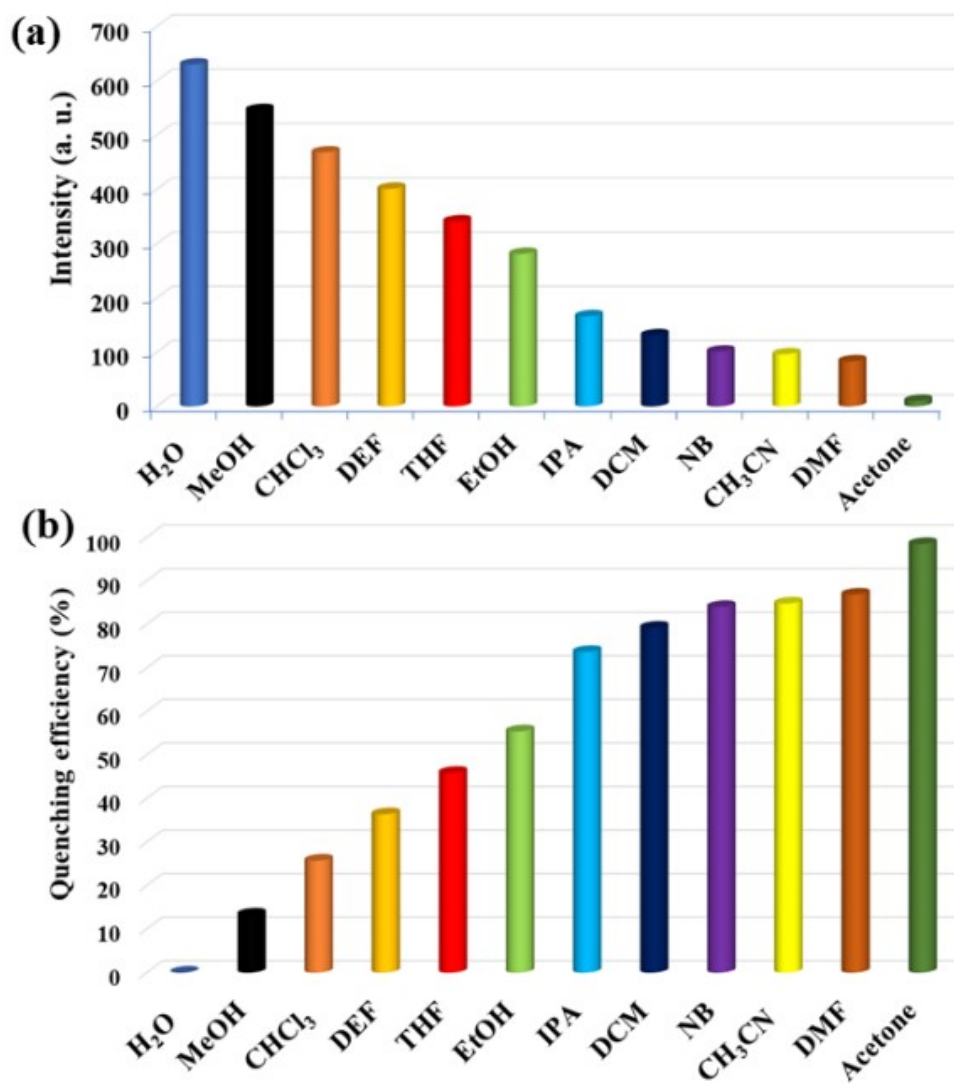


Fig. S2 For Fe@Zn-MOF-2 (a) Fluorescence intensity levels (b) quenching efficiencies, when numerous solvents are introduced when excited at 300 nm.

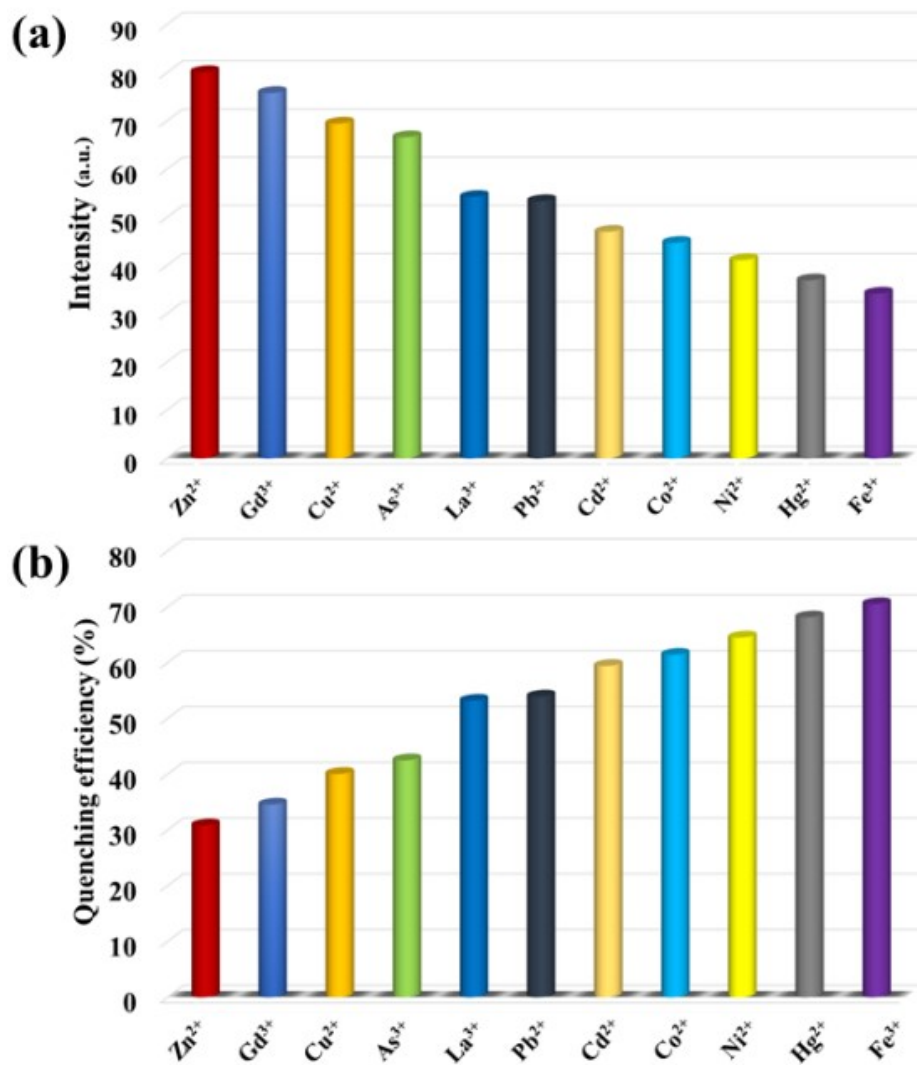


Fig. S3 Fluorescence intensity levels and quenching efficiency for Zn-MOF when various metal cations are introduced when excited at 300 nm.

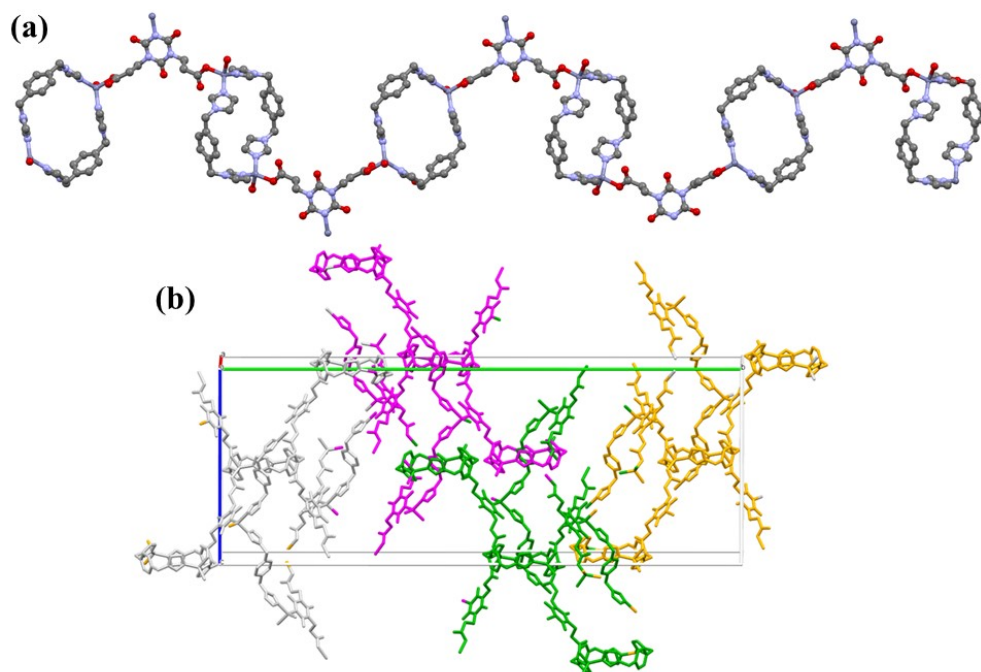


Fig. S4 (a) 1D zig-zag chain like structure along with a-axis. (b) Unit cell representation of $[\text{Zn}_9(\text{Cei})_6(\text{Bimb})_9]_n$ (**Zn-MOF**).

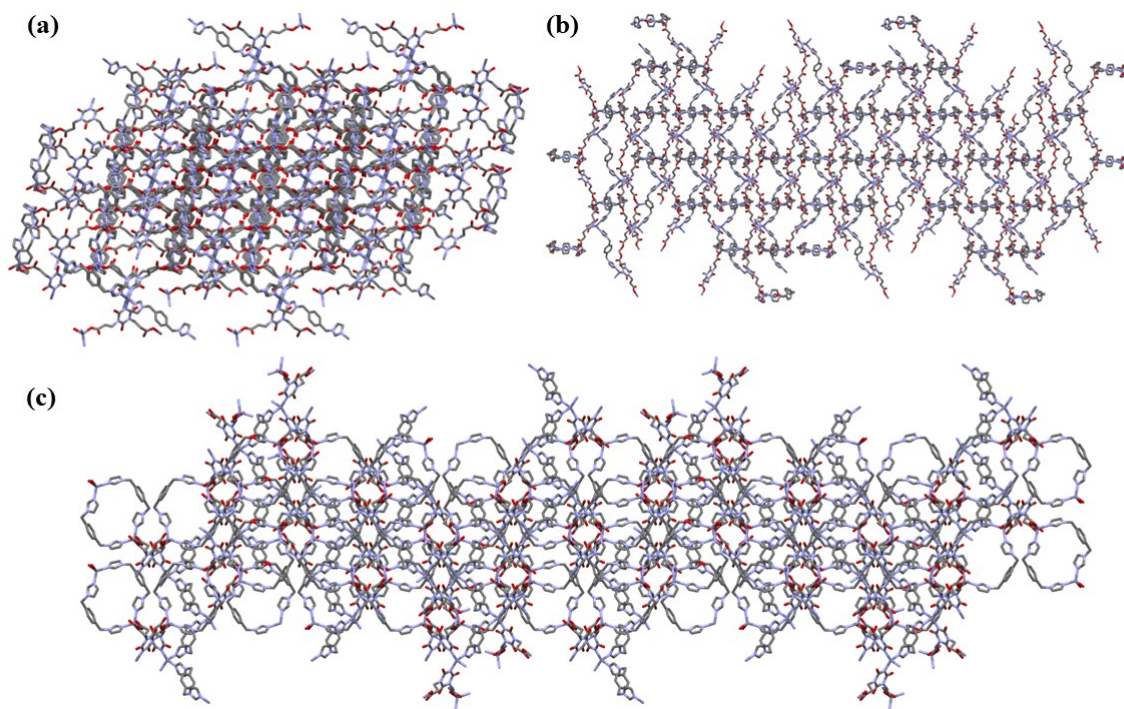


Fig. S5 2D structural representation of $[\text{Zn}_9(\text{Cei})_6(\text{Bimb})_9]_n$ (**Zn-MOF**) along with (a) b-axis (b) c-axis and (c) along with a-axis.

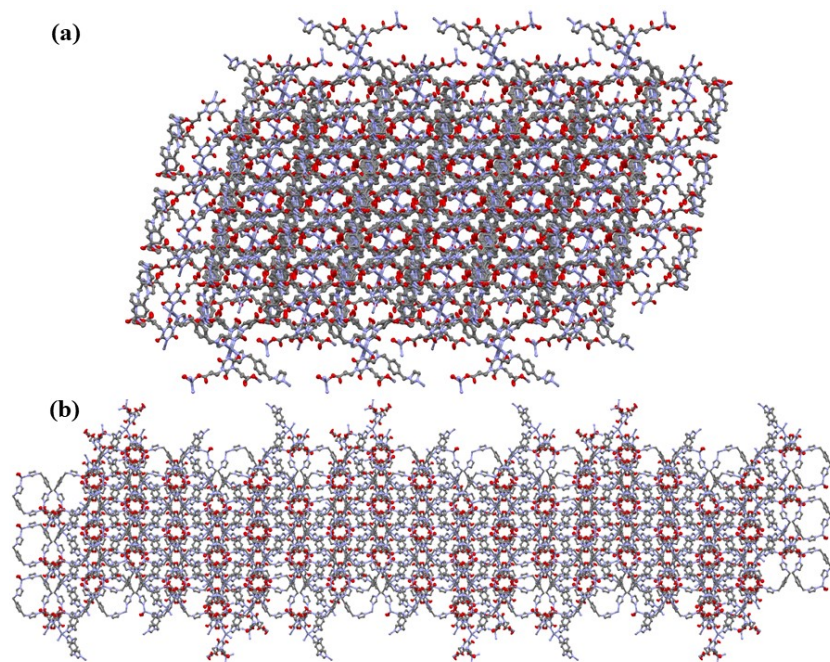


Fig. S6 Three-dimensional structural representation of $[Zn_9(Cei)_6(Bimb)_9]_n$ (**Zn-MOF**) along with (a) a-axis and (b) with b-axis.

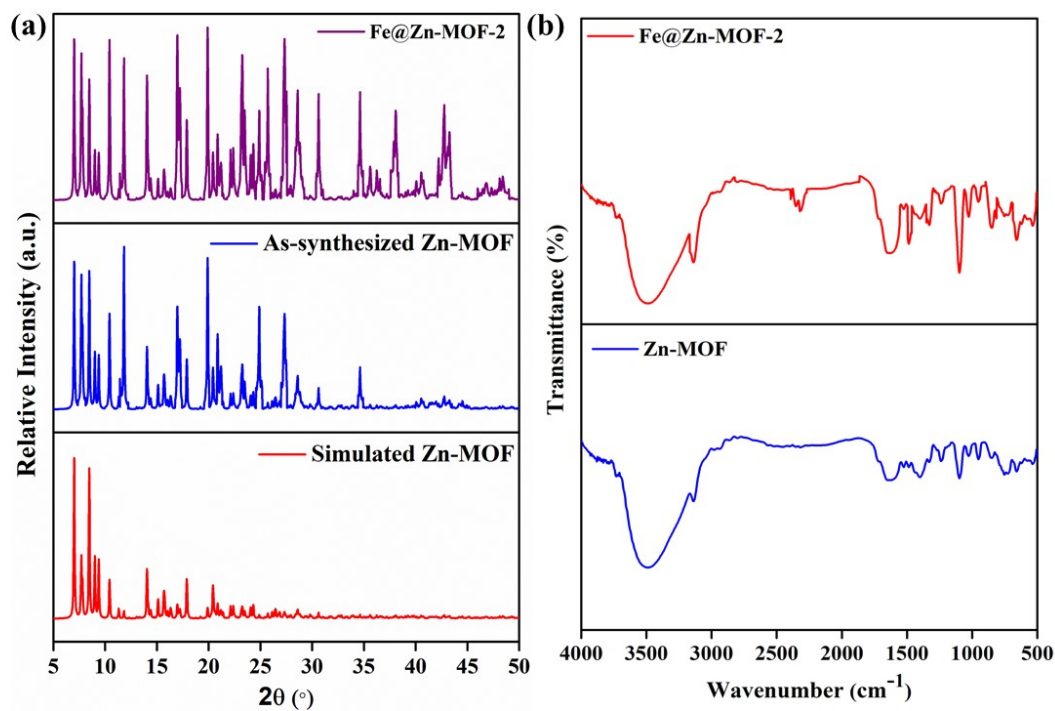


Fig. S7 (a) PXRD spectra of Zn-MOF as-synthesized, simulated and Fe@Zn-MOF-2 (b) FTIR spectra of Zn-MOF and Fe@Zn-MOF-2.

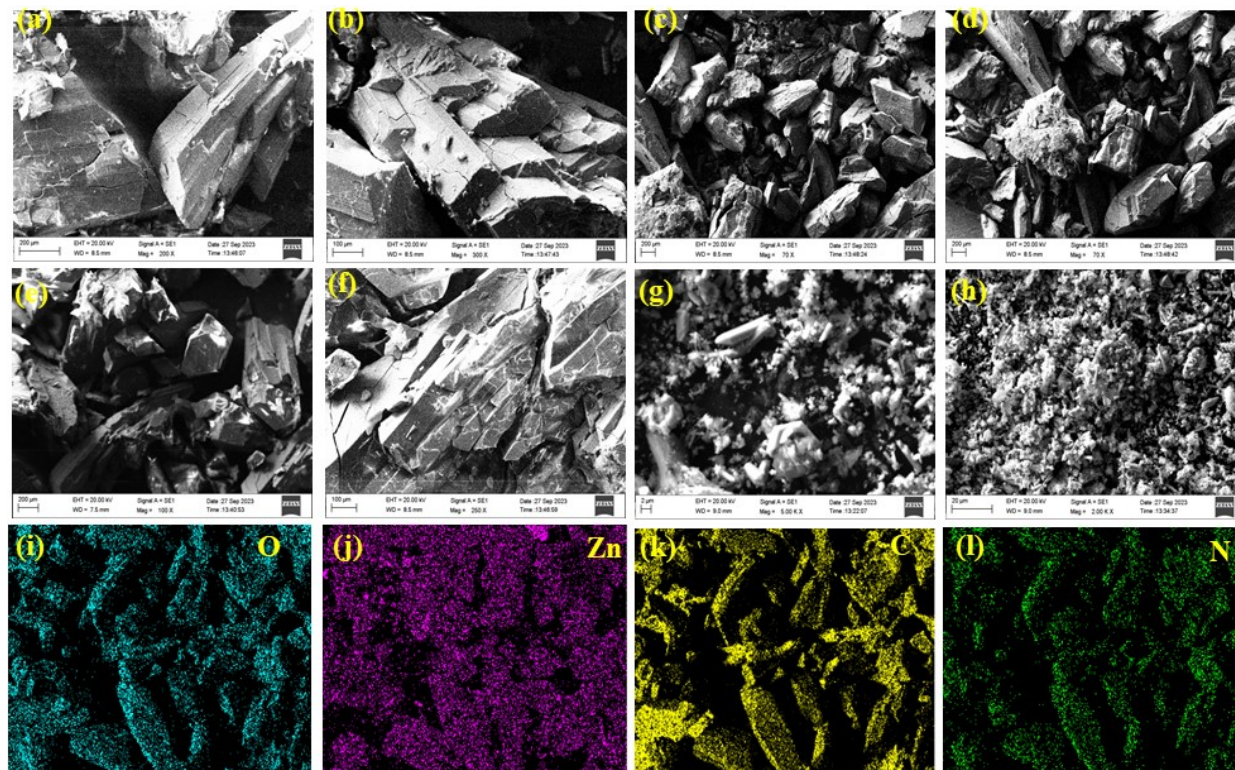


Fig. S8 SEM images of (a-f) $[\text{Zn}_9(\text{Cei})_6(\text{Bimb})_9]_n$ (Zn-MOF), (g-h) Zinc oxide nanoparticles at different magnification and (i-l) elemental mapping of (Zn-MOF).

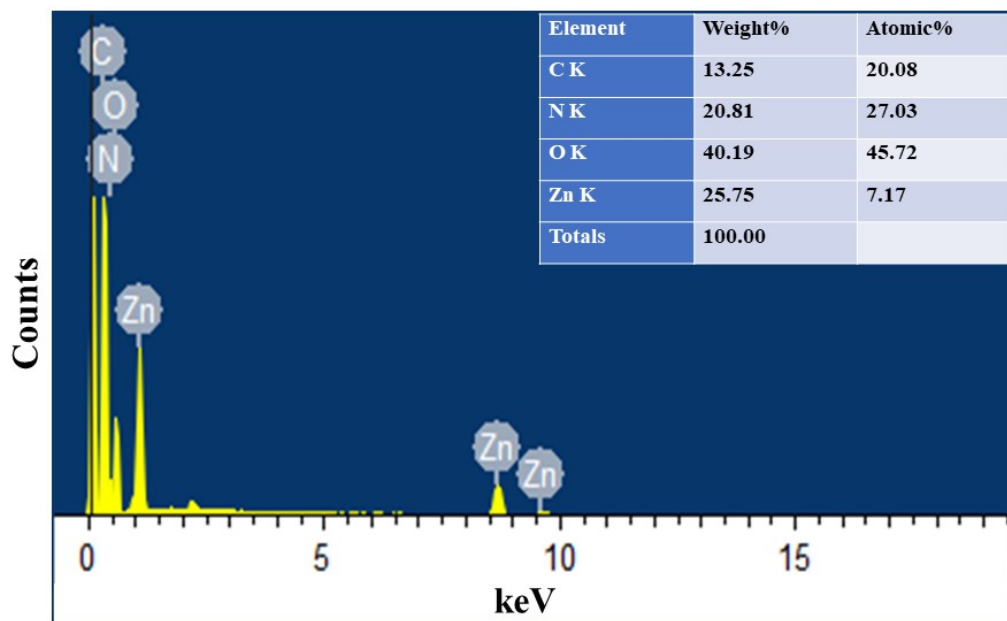


Fig. S9 EDAX analysis of $[\text{Zn}_9(\text{Cei})_6(\text{Bimb})_9]_n$ (Zn-MOF).

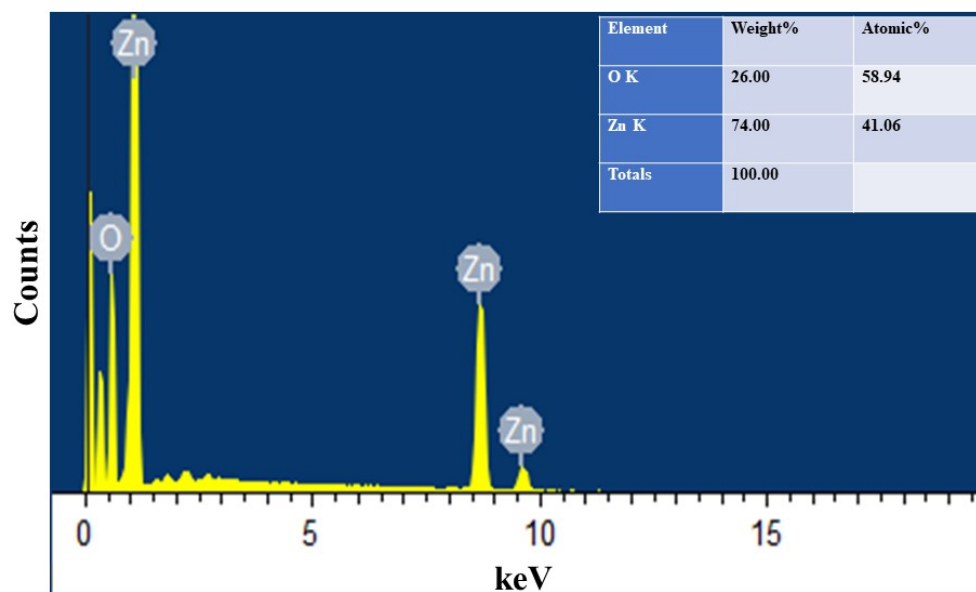


Fig.S10 EDAX analysis of Zinc-oxide nanoparticles.

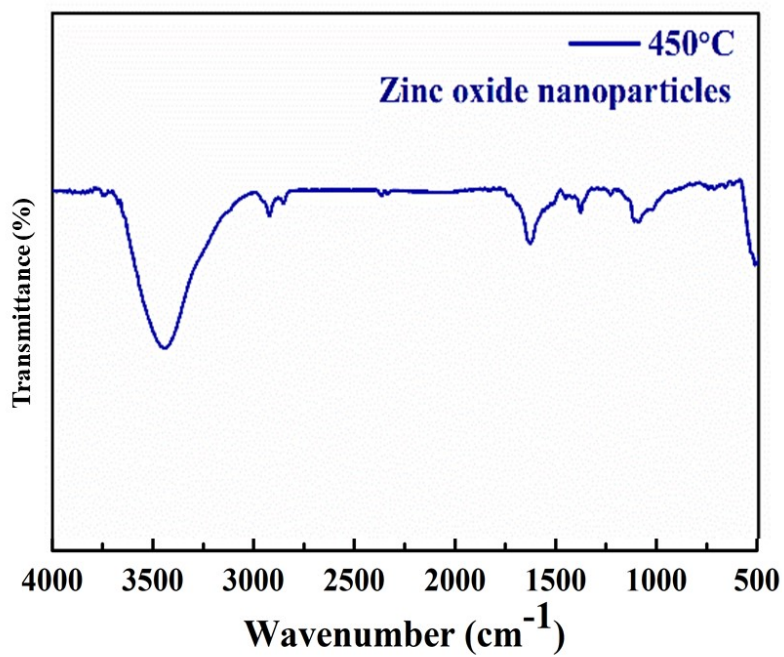


Fig. S11 FTIR spectra of Zinc-oxide nanoparticles.

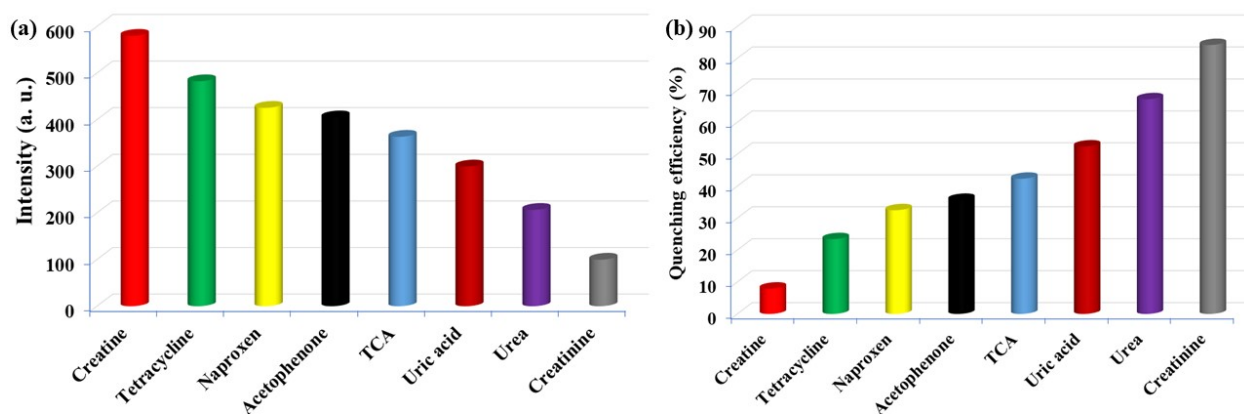


Fig. S12 (a) The relative emission intensity of **Zn-MOF** after immersing the as-synthesized sample into various pure biomarkers and antibiotics when excited at 300 nm. (b) Comparing the fluorescence quenching efficiencies of **Zn-MOF** when introducing in different biomarkers and antibiotics in aqueous solutions.

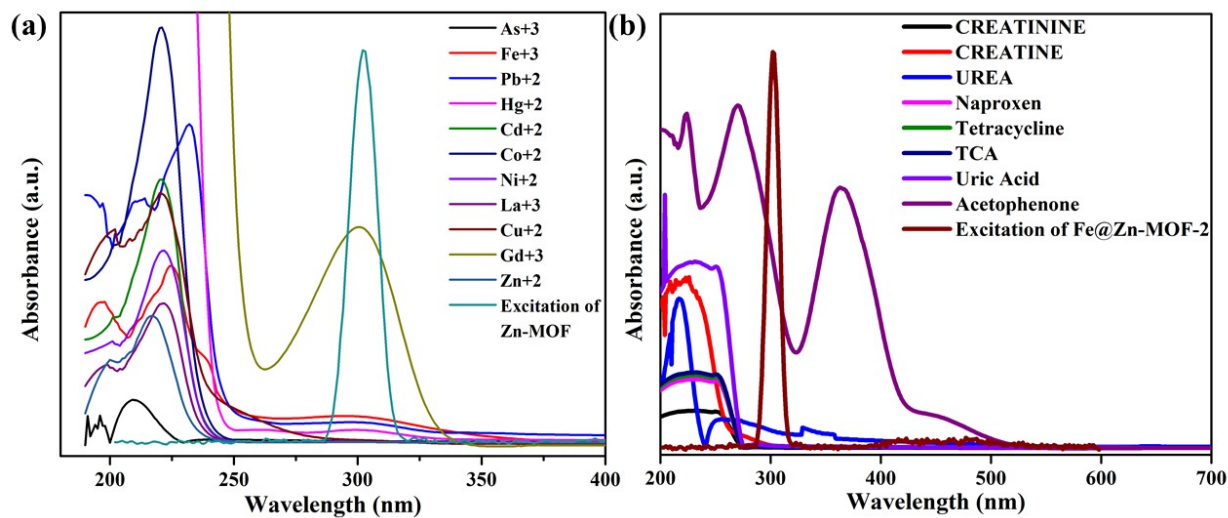


Fig. S13 Spectral overlap between the UV-Vis absorption spectra of various analytes (a) metal cations (b) biomarkers and the excitation spectra of **Fe@Zn-MOF-2**.

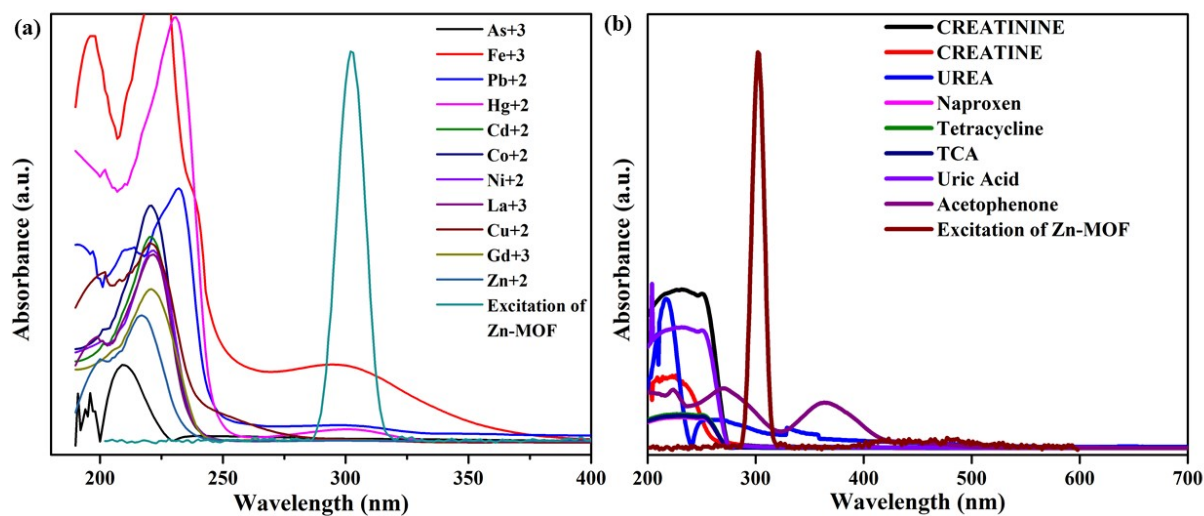


Fig. S14 Spectral overlap between the UV-Vis absorption spectra of various analytes and the excitation spectra of **Zn-MOF**.

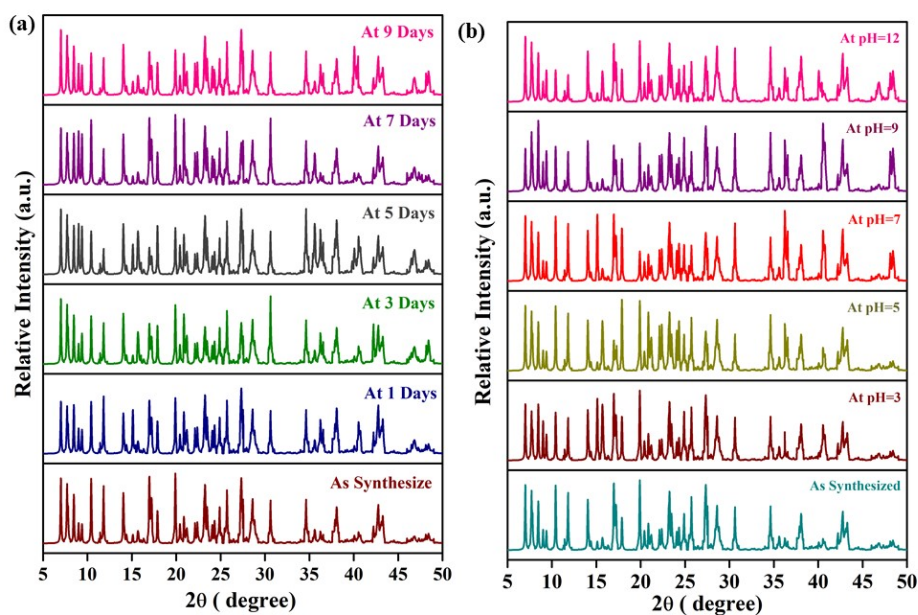


Fig. S15 PXRD spectra of Fe@Zn-MOF-2 (a) after removing from water (b) in different pH solution.

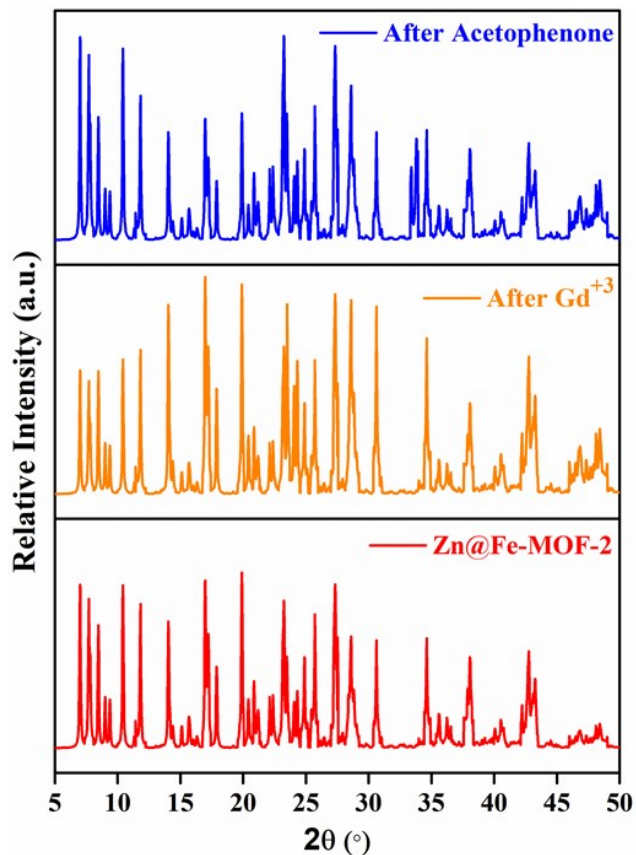


Fig. S16 PXR D spectra of Fe@Zn-MOF after sensing experiment.

Table. S1 Crystal Structure data and structural refinement data for $[\text{Zn}_9(\text{Cei})_6(\text{Bimb})_9]_n$ (Zn-MOF).

Identification Code	$[\text{Zn}_9(\text{Cei})_6(\text{Bimb})_9]_n$
Empirical formula	$\text{C}_{180}\text{H}_{174}\text{N}_{54}\text{O}_{42}\text{Zn}_9$ [+Solvent]
Formula weight	4354.05
Temperature/K	293 K
Crystal system	Monoclinic
Space group	$\text{P2}_1/\text{n}$
$a/\text{\AA}$	13.6442(1)
$b/\text{\AA}$	68.8042(5)
$c/\text{\AA}$	25.8089(1)
$\alpha/^\circ$	90
$\beta/^\circ$	102.409(1)
$\gamma/^\circ$	90
Volume/ \AA^3	23662.8(3)
Z	4
$\rho_{\text{calc}}/\text{g/cm}^3$	1.223
μ/mm^{-1}	1.61
F(000)	8952.0

Crystal size/mm³	0.390 × 0.230 × 0.170
Radiation	Cu Kα (λ = 1.54184)
2θ range for data collection/°	3.734 to 136.57
Index ranges	-11 ≤ h ≤ 16, -82 ≤ k ≤ 82, -31 ≤ l ≤ 30
Reflections collected	231011
Independent reflections	43002 [R _{int} = 0.0354, R _{sigma} = 0.0283]
Data/restraints/parameters	43002/0/2567
Goodness-of-fit on F²	1.063
Final R indexes [I>=2σ (I)]	R ₁ = 0.0623, wR ₂ = 0.1856
Final R indexes [all data]	R ₁ = 0.0770, wR ₂ = 0.1978
Largest diff. peak/hole / e Å⁻³	1.50/-0.68
CCDC No.	2339587

Table S2: Selected bond lengths of Zn-MOF(Å).

Zn1—O39 ⁱ	1.961 (2)
Zn1—N19	1.988 (2)
Zn1—N30	1.998 (3)
Zn1—O13	2.012 (2)
Zn2—O38	1.948 (2)
Zn2—N54	1.987 (2)
Zn2—N26	1.998 (3)
Zn2—O29	2.025 (3)
Zn3—O8	1.964 (2)
Zn3—O40	1.9767 (19)
Zn3—N44	1.983 (2)
Zn3—N16	1.998 (2)
Zn4—O15	1.971 (2)

Zn4—O5	1.974 (2)
Zn4—N20	1.990 (2)
Zn4—N22	2.000 (2)
Zn5—N32	2.000 (2)
Zn5—N6 ⁱⁱ	2.001 (2)
Zn5—N11	2.030 (2)
Zn5—N12	2.034 (2)
Zn6—N23 ⁱⁱⁱ	2.002 (2)
Zn6—N3	2.008 (2)
Zn6—N13 ^{iv}	2.031 (2)
Zn6—N17 ^v	2.033 (2)
Zn7—O30 ^{vi}	1.963 (3)
Zn7—O42	1.971 (2)
Zn7—N15	1.987 (2)
Zn7—N25	1.999 (2)
Zn8—O6	1.938 (3)
Zn8—N50 ^{vii}	1.986 (2)
Zn8—N31 ^{vii}	2.000 (3)
Zn8—O20 ⁱ	2.021 (3)
Zn9—N14 ^{viii}	1.998 (2)
Zn9—N7	2.001 (2)
Zn9—N49	2.023 (2)
Zn9—N24	2.037 (2)

Symmetry Element of Zn-¹-1-X,-Y,1-Z; ²1+X,+Y,-1+Z; ³1+X,+Y,1+Z; ⁴3/2+X,1/2-Y,1/2+Z;
⁵1/2+X,1/2-Y,1/2+Z; ⁶+X,+Y,-1+Z; ⁷-1+X,+Y,1+Z; ⁸2-X,-Y,2-Z; ⁹1-X,-Y,2-Z; ¹⁰-3/2+X,1/2-Y,-
1/2+Z; ¹¹-1/2+X,1/2-Y,-1/2+Z; ¹²+X,+Y,1+Z

Table S3: Selected bond Angles of Zn-MOF(°).

O39 ⁱ —Zn1—N19	110.03 (10)
---------------------------	-------------

O39 ⁱ —Zn1—N30	108.99 (10)
N19—Zn1—N30	117.16 (10)
O39 ⁱ —Zn1—O13	95.53 (10)
N19—Zn1—O13	110.34 (10)
N30—Zn1—O13	112.62 (11)
O38—Zn2—N54	111.21 (11)
O38—Zn2—N26	108.59 (11)
N54—Zn2—N26	116.87 (10)
O38—Zn2—O29	95.27 (12)
N54—Zn2—O29	110.24 (11)
N26—Zn2—O29	112.55 (12)
O8—Zn3—O40	94.06 (9)
O8—Zn3—N44	114.86 (10)
O40—Zn3—N44	108.83 (9)
O8—Zn3—N16	107.21 (10)
O40—Zn3—N16	113.58 (9)
N44—Zn3—N16	116.27 (10)
O15—Zn4—O5	93.39 (10)
O15—Zn4—N20	113.71 (11)
O5—Zn4—N20	109.11 (10)
O15—Zn4—N22	108.00 (11)
O5—Zn4—N22	114.31 (10)
N20—Zn4—N22	116.17 (10)
N32—Zn5—N6 ⁱⁱ	118.40 (11)
N32—Zn5—N11	122.39 (9)
N6 ⁱⁱ —Zn5—N11	98.45 (9)
N32—Zn5—N12	97.51 (10)
N6 ⁱⁱ —Zn5—N12	121.34 (9)
N11—Zn5—N12	98.73 (10)
N23 ⁱⁱⁱ —Zn6—N3	118.53 (11)

N23 ⁱⁱⁱ —Zn6—N13 ^{iv}	98.43 (10)
N3—Zn6—N13 ^{iv}	122.41 (10)
N23 ⁱⁱⁱ —Zn6—N17 ^v	121.39 (9)
N3—Zn6—N17 ^v	97.26 (10)
N13 ^{iv} —Zn6—N17 ^v	98.82 (10)
O30 ^{vi} —Zn7—O42	92.85 (12)
O30 ^{vi} —Zn7—N15	114.46 (11)
O42—Zn7—N15	109.47 (11)
O30 ^{vi} —Zn7—N25	107.21 (11)
O42—Zn7—N25	114.28 (11)
N15—Zn7—N25	116.30 (10)
O6—Zn8—N50 ^{vii}	110.80 (11)
O6—Zn8—N31 ^{vii}	108.92 (12)
N50 ^{vii} —Zn8—N31 ^{vii}	117.28 (10)
O6—Zn8—O20 ⁱ	95.18 (14)
N50 ^{vii} —Zn8—O20 ⁱ	109.57 (11)
N31 ^{vii} —Zn8—O20 ⁱ	112.89 (12)
N14 ^{viii} —Zn9—N7	118.42 (11)
N14 ^{viii} —Zn9—N49	122.04 (10)
N7—Zn9—N49	97.92 (10)
N14 ^{viii} —Zn9—N24	97.81 (10)
N7—Zn9—N24	121.82 (10)
N49—Zn9—N24	98.88 (11)
C19—O5—Zn4	112.1 (2)
C89—O6—Zn8	119.1 (3)
C59—O8—Zn3	121.2 (2)
C97—O13—Zn1	110.4 (2)
C94—O15—Zn4	122.0 (2)
C126—O20—Zn8 ^{vi}	110.2 (3)
C119—O29—Zn2	108.9 (3)

C99—O30—Zn7 ⁱ	120.5 (2)
C102—O38—Zn2	117.0 (2)
C153—O39—Zn1 ^{vi}	117.5 (2)
C5—O40—Zn3	113.18 (19)
C54—O42—Zn7	111.4 (2)
C9—N6—Zn5 ⁱⁱ	122.6 (2)
C10—N6—Zn5 ⁱⁱ	115.77 (17)
C60—N7—C33	122.0 (3)
C60—N7—Zn9	122.0 (2)
C33—N7—Zn9	115.73 (18)
C30—N11—Zn5	132.2 (2)
C55—N11—Zn5	121.3 (2)
C14—N12—Zn5	132.0 (2)
C82—N12—Zn5	121.4 (2)
C32—N13—Zn6 ^x	132.2 (2)
C75—N13—Zn6 ^x	121.4 (2)
C64—N14—Zn9 ^{viii}	121.2 (2)
C24—N14—Zn9 ^{viii}	116.45 (19)
C2—N15—Zn7	125.0 (2)
C144—N15—Zn7	128.5 (2)
C11—N16—C147	105.4 (2)
C11—N16—Zn3	129.1 (2)
C147—N16—Zn3	125.5 (2)
C25—N17—Zn6 ^{xi}	132.1 (2)
C74—N17—Zn6 ^{xi}	121.5 (2)
C3—N19—Zn1	126.4 (2)
C42—N19—Zn1	127.6 (2)
C6—N20—Zn4	124.6 (2)
C137—N20—Zn4	128.27 (19)
C8—N22—Zn4	129.1 (2)

C65—N22—Zn4	125.1 (2)
C37—N23—Zn6 ⁱⁱⁱ	122.1 (2)
C26—N23—Zn6 ⁱⁱⁱ	115.82 (18)
C57—N24—Zn9	132.2 (2)
C164—N24—Zn9	121.3 (2)
C50—N25—Zn7	129.0 (2)
C162—N25—Zn7	125.2 (2)
C53—N26—Zn2	127.6 (2)
C120—N26—Zn2	126.2 (2)
C49—N30—Zn1	127.4 (2)
C104—N30—Zn1	126.3 (2)
C29—N31—Zn8 ^{xii}	128.1 (2)
C92—N31—Zn8 ^{xii}	126.2 (2)
C12—N32—Zn5	120.8 (2)
C16—N32—Zn5	116.49 (18)
C28—N49—Zn9	132.0 (2)
C163—N49—Zn9	121.8 (2)
C13—N50—Zn8 ^{xii}	126.0 (2)
C46—N50—Zn8 ^{xii}	127.8 (2)

Symmetry Element of Zn-¹-1-X,-Y,1-Z; ²1+X,+Y,-1+Z; ³1+X,+Y,1+Z; ⁴3/2+X,1/2-Y,1/2+Z;
⁵1/2+X,1/2-Y,1/2+Z; ⁶+X,+Y,-1+Z; ⁷-1+X,+Y,1+Z; ⁸2-X,-Y,2-Z; ⁹1-X,-Y,2-Z; ¹⁰-3/2+X,1/2-Y,-
1/2+Z; ¹¹-1/2+X,1/2-Y,-1/2+Z; ¹²+X,+Y,1+Z

Table S4 Comparison of LOD values of Fe@Zinc-MOF-2 and previously reported materials.

S. No.	Material	Analyte	LOD	Ref.
1.	AuNP@BSPP	Gd ⁺³	0.74 mM	1.

2.	Gd-based contrasting agents	Gd ⁺³	0.40–20 mM	2.
3.	GdDTPA-BMA	Gd ⁺³	0.3 mM (serum), 1.1 mM (urine)	3.
4.	Gadodiamide	Gd ⁺³	1.9 mM (ICP-AES of serum)	4.
5.	Gd-based contrasting agents	Gd ⁺³	0.1–1 mM	5.
6.	Gd-based contrasting agents	Gd ⁺³	0.05–0.2 mM	6.
7.	Pr ₆ O ₁₁	Acetophenone	0.7 ppm	7.
8.	Fusion protein	Acetophenone	50 μM to 250 μM	8.
9.	Ionic liquids	Acetophenone	1.0 to 4.7 ppm	9.
10.	Fe@Zinc-MOF-2	Gd ⁺³ Acetophenone	0.204 ppm 0.192 ppm	This work

References –

1. M. Yon, C. Pibourret, J.-D. Marty and D. Ciuculescu-Pradines, *Nanoscale Adv.*, 2020, **2**, 4671–4681.
2. M. Andr'asi, A. G'asp'ar, O. Kov'acs, Z. Baranyai, A. Klekner and E. Br'ucher, *Electrophoresis*, 2011, **32**, 2223–2228.
3. E. Hvattum, P. T. Normann, G. C. Jamieson, J.-J. Lai and T. Skotland, *J. Pharm. Biomed. Anal.*, 1995, **13**, 927–932.
4. P. T. Normann, P. Joffe, I. Martinsen and H. S. Thomsen, *J. Pharm. Biomed. Anal.*, 2000, **22**, 939–947.

5. J. Künemeyer, L. Terborg, S. Nowak, A. Scheffer, L. Telgmann, F. Tokmak, A. Günzel, G. Wiesmüller, S. Reichelt and U. Karst, *Anal. Chem.*, 2008, **80**, 8163–8170.
6. C. L. Kahakachchi and D. A. Moore, *J. Anal. At. Spectrom.*, 2009, **24**, 1389.
7. Q.-C. Zhang, W.-L. Yan, L. Jiang, Y.-G. Zheng, J.-X. Wang and R.-K. Zhang, *Molecules*, 2019, **24**, 4275.
8. E. Muhr, O. Leicht, S. González Sierra, M. Thanbichler and J. Heider, *Front. Microbiol.*, 2015, **6**, 1561.
9. J. Gębicki, A. Kloskowski and W. Chrzanowski, *Sens. Actuators B Chem.*, 2013, **177**, 1173–1179.